INL/CON-12-27560
PREPRINT

Multicomponent Equilibrium Models for Testing Geothermometry Approaches

38th Workshop on Geothermal Reservoir Engineering

D. Craig Cooper
Carl D. Palmer
Robert W. Smith
Travis L. McLing

February 2013

The INL is a
U.S. Department of Energy
National Laboratory
operated by
Battelle Energy Alliance

PROCEEDINGS, Thirty-Eighth Workshop on Geothermal Reservoir Engineering
Stanford University, Stanford, California, February 11-13, 2013
SGP-TR-198

MULTICOMPONENT EQUILIBRIUM MODELS FOR TESTING GEOTHERMOMETRY APPROACHES

D. Craig Cooper[1], Carl D. Palmer[1], Robert W. Smith[2,3], and Travis L. McLing[1,3], and

[1]Idaho National Laboratory, Idaho Falls, ID, 83415, USA

[2]University of Idaho-Idaho Falls, Idaho Falls, ID, 83402, USA

[3]Center for Advanced Energy Studies, Idaho Falls, ID, 83415, USA

e-mail: craig.cooper@inl.gov

ABSTRACT

Geothermometry is an important tool for estimating deep reservoir temperature from the geochemical composition of shallower and cooler waters. The underlying assumption of geothermometry is that the waters collected from shallow wells and seeps maintain a chemical signature that reflects equilibrium in the deeper reservoir. Many of the geothermometers used in practice are based on correlation between water temperatures and composition or using thermodynamic calculations based a subset (typically silica, cations or cation ratios) of the dissolved constituents. An alternative approach is to use complete water compositions and equilibrium geochemical modeling to calculate the degree of disequilibrium (saturation index) for large number of potential reservoir minerals as a function of temperature. We have constructed several "forward" geochemical models using The Geochemist's Workbench to simulate the change in chemical composition of reservoir fluids as they migrate toward the surface. These models explicitly account for the formation (mass and composition) of a steam phase and equilibrium partitioning of volatile components (e.g., CO_2, H_2S, and H_2) into the steam as a result of pressure decreases associated with upward fluid migration from depth. We use the synthetic data generated from these simulations to determine the advantages and limitations of various geothermometry and optimization approaches for estimating the likely conditions (e.g., temperature, pCO_2) to which the water was exposed in the deep subsurface. We demonstrate the magnitude of errors that can result from boiling, loss of volatiles, and analytical error from sampling and instrumental analysis. The estimated reservoir temperatures for these scenarios are also compared to conventional geothermometers. These results can help improve estimation of geothermal resource temperature during exploration and early development.

INTRODUCTION

A major barrier to the deployment of geothermal energy is the financial risk associated with geothermal prospecting (U.S. DOE, 2011). Geophysical surveys and test wells are expensive, and advances in prospecting are needed to reduce risk and increase the return on prospecting investments. One possibility is to improve the accuracy of geothermometry by taking advantage of advances in geochemical analyses and modeling. In geothermal systems, physical processes (e.g., mixing, boiling) and geochemical processes (e.g., mineral dissolution, precipitation) along flow paths commonly alter the composition of migrating waters. If these changes are not accurately characterized and quantified, predictions of *in-situ* reservoir conditions (e.g., temperature, pCO_2) based on the chemical composition of sampled thermal waters may be erroneous, or too imprecise to be useful. However, if these processes can be correctly described and their impact on geothermometers quantified, the conditions in a deep reservoir temperature can be estimated with greater confidence.

The technical literature provides many examples of how geochemical modeling that simultaneously considers multiple mineral equilibria can be used to estimate the temperature of reservoir fluids from their geochemical fingerprints (e.g., Bethke 2008; Reed

and Spycher, 1984; Spycher et. al., 2011). However, this technique has not yet been widely adopted by the exploration industry, and most geothermometry is conducted using traditional approaches such as silica, Na-K, Na-K-Ca, Na-K-Ca-Mg, Na-Li, and K-Mg, and various gases and stable isotopes (e.g., Armannsson and Fridriksson, 2009; Karingithi, 2010, Young et. al., 2012). These approaches are useful, but suffer from some inherent limitations, including:

- Each of these geothermometers has a different conceptual model, and reliable selection of a geothermometer requires *a priori* knowledge of *in-situ* conditions.
- Because of this disparate set of conceptual models, each geothermometer will often predict a different temperature for the same solution chemistry.
- They do not provide for a straightforward method to independently assess the accuracy and/or reliability of the temperature prediction.
- They do not directly account for changes in fluid chemistry that occur as the fluid migrates from the reservoir to the sampling point that are the result of boiling and subsequent venting of volatile components even if no net heat (enthalpy) is lost.
- They do not explicitly account for the multiple influences of mineral alteration reactions on solution chemistry in a manner that allows for improvements in thermodynamic datasets and analytical technologies to be easily adopted.

Many of these weaknesses can be addressed if geochemical reaction path modeling is used as a basis for geothermometry. Modern geochemical models couple up-to-date thermodynamic datasets with user-provided aqueous solution and gas-phase composition to rapidly calculate the temperature-dependent saturation states of a fluid with hundreds of different minerals. These calculations, coupled with inverse parameter optimization, can be used to estimate reservoir temperature by determining the point at which multiple equilibria "converge" to a common temperature.

In this paper, we outline some of the concepts for a multicomponent equilibrium approach to geothermometry and discuss how these concepts can be implemented. The potential validity of this approach is tested using simulated datasets of synthetic geothermal waters that have a known reservoir temperature and hydrogeochemical history. We use that dataset to test an inverse numerical optimization approach for estimating geothermal reservoir temperatures using multicomponent equilibrium geothermometry.

MULTICOMPONENT GEOTHERMOMETRY

A simple conceptual model of a geothermal system is illustrated in Figure 1. While different sites have unique, site-specific aspects, the base conceptual model captures key chemical and physical features common to most geothermal systems.

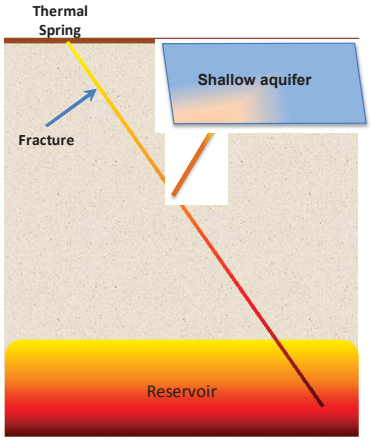

Figure 1: Conceptual model for geothermal system. Water and steam rising up to a thermal spring or shallow aquifer, experiencing cooling and venting of volatile components.

In this conceptual model, fluids in a deep reservoir are heated to reservoir temperature and react with the reservoir mineral assemblage. Equilibrium is assumed because the rates of reaction are expected to be relatively fast at these elevated temperatures. These geothermal waters then rise along a fracture, pressure drops and a portion of the water separates into a vapor phase (Figure 2).

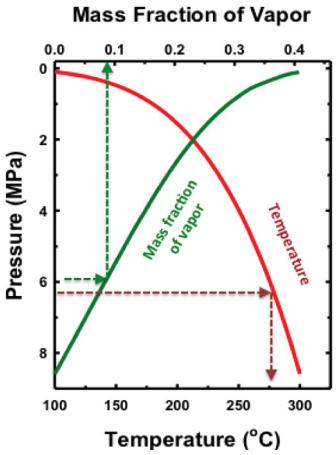

Figure 2: Pressure versus temperature (red line, bottom axis) and pressure versus mass fraction of vapor (green line, top axis) for water in constant enthalpy system.

This process also reduces fluid temperature, even though the total combined enthalpy of the fluids remains constant due to the latent heat of vaporization. The resulting two-phase system concentrates the non-volatile constituents in the liquid phase and partitions volatile components such as CO_2, CH_4, H_2, and H_2S to a steam phase; altering solution pH and redox (Eh) and shifting the saturation state for mineral equilibria. Near the surface, the geothermal system subsequently vents volatile components to the atmosphere (spring or well), or mixes with shallow groundwater (e.g., aquifer mixing). These cooler waters, or a steam condensate, are typically sampled during geothermal exploration and then analyzed for their mass and/or isotopic composition. The geochemical data collected from these samples are then used to estimate the temperature of the fluid in the deep reservoir, based on the assumption that the relatively slow rates of mineral dissolution and precipitation reactions at the lower temperatures along the migration path allow the solution to retain the geochemical fingerprint of the deep reservoir.

Some of the basic concepts of multicomponent geothermometry of been described by others (e.g., Bethke 2008; Reed and Spycher, 1984; Spycher et. al., 2011). The methodology involves calculating saturation indices of the near-surface water sample as a function of temperature. The reservoir temperature can then be defined as the *temperature at which the multiple mineral species deemed likely to be present in the system are in equilibrium with the solution composition, when mineral saturation states are plotted as a function of temperature*. This definition is depicted in the following example (Bethke, 2008).

A brine containing 3 molal Cl and 0.05 molal Ca at pH 5 is equilibrated with quartz, calcite, albite, K-spar, and muscovite at 250°C. This geothermal water is transported to the surface where the gas phase is condensed and reconstituted with the liquid phase at 25°C and the pH and dissolved constituents are measured. The system represents a closed hydrothermal system where both the liquid phase and the gas phase could be sampled. Speciation calculations are made at 25°C, at the pH measured at that temperature. The water is then speciated as a function of temperature over the range of 25°C to 300°C, allowing the pH to be calculated using The Geochemist's Workbench® (Version 9). Plotting the calculated mineral saturation indices as a function of temperature (Figure 3) shows that the indices for quartz, calcite, albite, K-feldspar, and muscovite converge common point where Q/K = 1 (log (Q/K) = 0) at 250 °C. This point where the saturation indices converge to zero is the reservoir temperature estimated by the multicomponent geothermometry approach. This estimate is identical to that used to generate the subsurface fluid chemistry in this simple example. However, real-world systems are more complex than this idealized example, and additional processes will need to be considered.

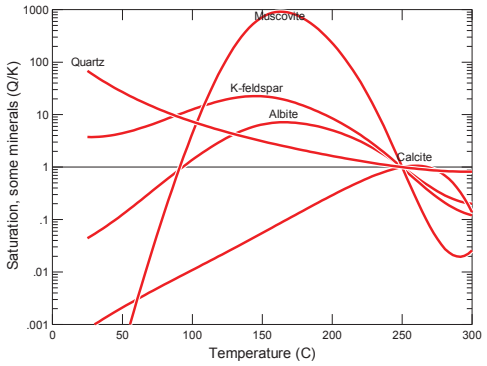

Figure 3: Plot of mineral saturation state versus temperature for a hypothetical closed geothermal system (Bethke, 2008).

For example, consider Figure 4, which shows how the system depicted in Figure 3 would behave if CO_2 was lost to the atmosphere at the sampling location (e.g., a spring). Here, the mineral saturation plots for albite, K-feldspar, and quartz appear to converge, but calcite and muscovite do not. Further, the convergence of albite, K-feldspar and quartz suggests a reservoir temperature of about 256°C rather than 250°C. Even for these three minerals, the saturation occurs at 257.4, 256.0, and 249.8°C, respectively.

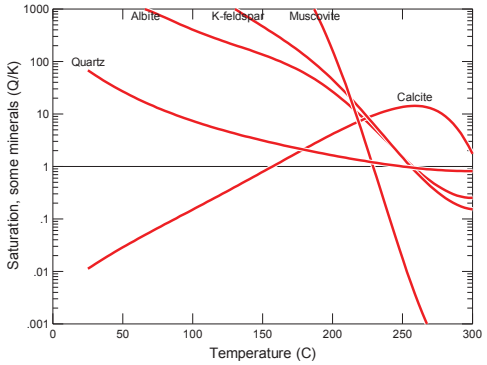

Figure 4: Plot of mineral saturation state versus temperature for the system depicted in Figure 3, but open to the atmosphere (Bethke, 2008).

This result clearly indicates that loss of volatile constituents from a geothermal system can have a significant impact on the relationship between fluid chemistry and estimated reservoir temperature. However, field sampling programs for geothermal exploration typically do not gather sufficient data to directly account for loss of volatile constituents. Thus, the optimization process should explicitly include volatile components lost (CO_2 in this case) as an optimization parameter.

In Figures 3 and 4, we have shown only the saturation indices of the minerals with which the initial reservoir fluid was equilibrated. It is important to note, however, that geochemical models can provide saturation indices for hundreds of mineral phases making graphical as well as numerical estimation of the reservoir extremely difficult, if not impossible. Fortunately, it is unnecessary and actually incorrect to include all potential solid phases in such calculations. For equilibrium, the Gibbs phase rule defines the maximum number of independent variables within a system (equation 1).

1. $F = C - P + 2$; *where*
   F = degrees of freedom (independent variables)
   C = number of components in system
   P = number of phases in system

For cases where there is a fluid phase present and system temperature and pressure are correlated (e.g., steam saturated water), the phase rule can be used to determine the maximum number of equilibrium phases that are appropriate for the calculation (equation 2).

2. $M = C - F$; *where*
   M = number of equilibrium minerals, and
   $M \leq C$

Although the Gibbs phase rule limits the number of minerals that can be considered, it does not tell us which minerals need to be included. Mineral selection represents an area of continuing uncertainty. The choice of minerals is dependent upon the reservoir lithology. The geoscience literature contains numerous studies that identify alteration mineral assemblages that form when hot water interacts with reservoir minerals (e.g., Schwartz, 1959). Many hydrothermal systems are equilibrated with the alteration mineral assemblages rather than the primary reservoir lithology (e.g., Bethke, 2008; Giggenbach, 1988). It is possible to conduct inverse numerical optimization calculations that test different feasible alteration mineral assemblages. However, this approach may not yield satisfactory results in cases where the number of minerals approaches or becomes equal to the number of independent constraints (i.e. compositional measurements). In this case, convergence to a common set and values for optimization parameter would become increasingly sensitive to inherent measurement errors. An alternative is to develop a dataset of commonly observed alteration mineral assemblages for a specific lithology at low, medium, or high reservoir temperature; and then select the appropriate mineral set – using the Gibbs Phase Rule for guidance in the number of minerals to consider. This would allow the analyst to conduct multiple calculations, using the same computational and conceptual basis, but with different input parameters; and then contrast results with available field data. The relative merits of these approaches should be assessed in future work.

Another challenge associated with geothermometry is accounting for uncertainty in geochemical analyses. The calculations associated with Figures 3 and 4 are based on idealized systems in which all the parameters were "measured" with perfect certainty. In reality, chemical analyses contain analytical errors that can contribute to the overall uncertainty in the estimation of the reservoir temperature. We need to better understand the magnitude of this uncertainty and develop methods that allow us in incorporate analytical uncertainty into the uncertainty in the estimates of reservoir temperature.

APPROACH

Geochemical Calculations

As we have discussed in the previous section, several factors need to be considered for improved geothermometry:

- Estimating the steam-water partitioning that occurs as geothermal fluids migrate from depth to the sampling location.
- Partitioning of volatiles between the gas and liquid phases
- Identifying the mineral phases that control water-rock equilibrium in the deep reservoir.
- Assessing the impact of analytical error on the estimates of reservoir temperature

With respect to steam-water partitioning, pressure reductions and cooling that occurs when fluids rise from deep geothermal systems alter the percentage of total water that is present as a liquid. For example, consider the trends in Figure 2, which depicts water partitioning in a closed, constant enthalpy system. At

8 MPa pressure, the system consists of ~2% steam and ~98% water at 300 °C. At constant total enthalpy, the same fluid at atmospheric pressure is ~40% steam and ~60% water and 100 °C. This partitioning will concentrate dissolved ions in water and facilitate the partitioning of volatile species in to the steam phase. Liquid water loss can be treated by two different approaches:

- For a general case; specifying a % mass loss of water due to vaporization.
- For a closed, constant enthalpy system; calculating the mass of water lost to the vapor phase along each temperature step

The mass loss of volatile species from solution (e.g., CO_2, H_2S) can be treated similarly. For the general case, the mass loss can be specified directly. For a closed, constant enthalpy system; mass loss of volatile components can be iteratively calculated. Both approaches use mass loss as an optimization parameter, but the closed system approach allows for calculations to be made for cases where the aqueous and gas phases may follow different paths. If volatile loss is calculated iteratively, a mass balance is performed over both phases as shown in equation 3.

3.

$$P_{k,k,g} = \frac{\rho_{H_2O,l} K_{H,k} \left[M_{k,total} - M^0_{H2O}(1 - X_{k,g}) \left(\sum_{\substack{i \\ i \neq k}} a_{i,k} C_{k,i,l} \right) \right]}{1000 \phi_k M^0_{H2O} \left[(1 - X_{k,g}) + \frac{X_{k,g} K_{H,k} \rho_{H_2O,l}}{RT \rho_{H_2O,g}} \right]}$$

where:

$P_{k,k,g}$ = partial pressure of the kth gas component,
$K_{H,k}$ = Henry's coefficient,
$\rho_{H2O,l}$ = density of liquid water,
$M_{k,total}$ = total mass of component k,
$X_{k,g}$ = mass fraction of water in the gas phase,
M^0_{H2O} = initial mass of water,
$\rho_{H2O,g}$ = density of the vapor phase,
ϕ_k = fugacity coefficient for gas component k
$C_{k,i,l}$ = molal concentrations of species i containing component k with stoichiometric coefficient a_{ik}.

We are currently testing both of these approaches for accounting for loss of water and volatile components. However, for this paper, we are demonstrating these concepts using the more general approach that does not require the assumption of a closed, constant enthalpy system.

Inverse Optimizations

For estimating the reservoir temperature, we use an optimization approach rather than the graphical approach illustrated in Figures 3 and 4. Ultimately, these calculations will be conducted by coupling The Geochemist's Workbench® (GWB) with the general parameter estimation and optimization code PEST (Doherty, 2005). However, for this paper we have done the calculations by iteratively applying GWB to generate a dataset of mineral saturation as a function of temperature and volatile constituents lost, and then finding the optimum solution for an objective function that indicates the system's overall mineral saturation state. We have defined our objective function as the minimization of the Total Saturation Index (TSI), shown in equation 4.

4. $TSI = \Sigma (SI_i / wt_i)^2$;

SI_i = log (Q_i/K_i) for the ith equilibrium mineral

wt_i = weighting factor based on the number of thermodynamic components (i.e., independent chemical variables) and the number of time each component appears in the ith mineral dissolution reaction.

Because of the squared term in Equation 4, TSI values are always greater than or equal to zero and can pass through both positive minima and maxima. The advantages of expressing the objective function in ways other than the Euclidean norm, will be explored in future work.

For a system in equilibrium and with no measurement errors, the overall equilibrium state occurs at the point at which TSI = 0. For real water samples subject to sampling and analytical errors, the TSI value should always be greater than zero. The weighting factor ensures that each mineral that contributes to the equilibrium state is considered equally and the results are not skewed by reaction stoichiometry. The weighting factors used in our calculations are based on writing the reactions so that a total of 1 mole of ions are added to solution. Weighting factors for some example minerals are provided in Table 1. Other weighting methods can also be used.

Table 1: Weighting factors for selected minerals.

Mineral	Thermodynamic Components	Weight factor
Albite	1*Al^{3+}, 1*Na^{+}, 3*SiO_2	5
Calcite	1*Ca^{2}, 1*CO_3^{2-}	2
K-feldspar	1*Al^{3+}, 1*K^{+}, 3*SiO_2	5
Muscovite	3*Al^{3+}, 1*K^{+}, 3*SiO_2	7
Quartz	1*SiO_2	1

Example Test Cases

To illustrate the potential power and limitations of the multicomponent equilibrium geothermometry approach, we have tested the inverse reaction path modeling approach against simulated data from four different geothermal scenarios. The scenarios were generated using The Geochemist's Workbench®, Version 9 (Bethke and Yeakel, 2011), using the thermo.dat thermodynamic database. These simulated numerical datasets assumed a reservoir mineral assemblage, equilibrated water with that assemblage at a given temperature, and then subjected the simulated deep waters to a sequence of thermal and chemical events (e.g., boiling, cooling venting). The computed water chemistry represents the chemistry of water collected from a thermal spring or sampling well. We also investigate the potential impacts of sampling errors.

For each case, the given solution chemistry was input into The Geochemist's Workbench®, and the log (Q/K) calculated as a function of temperature for a assumed equilibrium mineral assemblage of albite, calcite, K-feldspar, muscovite, and quartz were. The calculations were conducted for the range of 25°C to 300°C. The effect of mass loss of CO_2 due to volatilization was assessed by numerically adding CO_2(aq) back in to the solution at increments of 0.1 molal over the range of 1e-4 to 1.0 molal. In some cases, increments of 0.02 and 0.05 molal were also considered over the range of 1e-4 to 0.1 molal. For each case, these calculations yielded a dataset of TSI and temperature in increments of CO_2-added. This dataset was then used to estimate the both reservoir CO_2 and temperature by the condition at which TSI had its minimum value using the following process:

1. The optimum mass of CO_2 added (mol/kg) was determined by finding the minimum on a plot of TSI at dTSI/dT = 0 versus CO_2 added
2. The optimum temperature was determined by plotting temperature at dTSI/dT = 0 versus CO_2 added, and then determining the temperature at the point that corresponds to the optimum mass of CO_2 added.
3. The TSI at the optimum mass of CO_2 added was calculated similarly.

For cases where water was lost due to boiling, the impact of water loss was qualitatively assessed by conducting replicate calculations at different extents of water loss. The test cases are described below, and the associated solution chemistry is provided in Table 2.

Case 1: Open system (Bethke, 2008). A brine containing 3 molal Cl and 0.05 molal Ca at pH 5 is equilibrated with quartz, calcite, albite, K-spar, and muscovite at 250°C. This geothermal water is transported to the surface where the fluid cools to 25°C and CO_2 vents to the atmosphere. The system represents a geothermal water that has reached the surface, cooled under closed conditions and then was exposed to the atmosphere.

Case 2: Effect of Analytical Errors. This simulation is the same as Test Case 1 except that random errors are introduced into the data: 15% relative standard deviation for Al, 10 % for HCO_3^-, 5% for Ca, Cl, K, Na, SiO_2, 0.15 units for pH, and 1°C for temperature.

Case 3: Deep Boiling. A brine containing 3 molal Cl and 0.05 molal Ca at pH 5 is equilibrated with quartz, calcite, albite, K-spar, and muscovite at 250°C. This geothermal water is then isothermally boiled until 15% of the water is lost while maintaining equilibrium with the reservoir mineral assemblage. The resulting water is then transported to the surface where the fluid cools to 25°C and CO_2 vents to the atmosphere.

Case 4: Flashing. A brine containing 3 molal Cl and 0.05 molal Ca at pH 5 is equilibrated with quartz, calcite, albite, K-spar, and muscovite at 250°C. This geothermal water is then isothermally boiled until 15% of the water is lost but mineral reaction does not occur during boiling. The resulting water is then transported to the surface where the fluid cools to 25°C and CO_2 vents to the atmosphere. This scenario represents fluid flashing within a well.

Table 2: Solution Chemistry for Numerical Test Cases.

Case	Al^{3+} (mg/kg)	Ca^{2+} (mg/kg)	Na^+ (mg/kg)	K^+ (mg/kg)	Cl^- (mg/kg)	HCO_3^- (mg/kg)	SiO_2 (mg/kg)	pH	Sample Temp.
1	8.66 e-3	2.00 e3	6.39 e4	1.01 e4	1.13 e4	2.39 e3	2.10 e2	5.10	25 °C
2	9.53 e-3	1.96 e3	6.64 e4	0.98 e4	1.10 e4	2.20 e3	2.12 e2	5.09	24.4 °C
3	7.65 e-3	2.35 e3	7.66 e4	1.21 e4	1.33 e4	2.41 e3	2.07 e2	5.13	25 °C
4	10.2 e-3	2.36 e3	7.52 e4	1.19 e4	1.31 e4	0.85 e3	2.45 e2	5.20	25 °C

RESULTS

Results from the inverse geochemical calculations are summarized in Table 3. For the relatively simple scenario in Case 1, the inverse method independently predicted reservoir temperature to within ± 1 °C. This result is a significant improvement over the results gained when only temperature is considered (e.g., Figure 4), and demonstrates how including volatile loss as part of the optimization scheme can greatly improve geothermometry.

Table 3: Results from Inverse Calculations. For all cases, the actual temperature is 250 °C.

Case	H_2O loss	T (°C)	CO_2-aq added (mol/kg)	TSI at optimum
1	n.a.	250.6	0.52	5.12 e-4
2	n.a.	253.0	0.45	7.72 e-4
3	none	249.7	0.63	4.50 e-4
	10%	242.0	0.44	1.33 e-3
	20%	233.5	0.29	2.69 e-3
	30%	221.2	0.14	7.03 e-3
4	none	259.6	0.08	6.50 e-2
	10%	254.1	0.07	1.13 e-2
	20%	248.7	0.06	9.27 e-3
	30%	233.3	0.03	2.03 e-2

The influence of volatile loss is also seen in the plot of Total Saturation Index (TSI) versus potential reservoir temperature for each amount of CO_2 added (Figure 5). In this plot, the different colored curves correspond to different masses of CO_2-added back into the system. Each of these curves shows a minimum that corresponds with the "convergence point" of saturation indices that can be qualitatively identified from a plot of temperature versus the log (Q/K) for sets of minerals that are likely to be present in a reservoir. The minimum becomes more clearly resolved as CO_2 is added back into the system to account for venting.

The blue line in Figure 5 represents a fully vented system (e.g., as in Figure 4). The lines where greater than 0.3 mol/kg H_2O of CO_2-(aq) have been added back into the system represent the closed system – prior to loss of volatiles (e.g., as in Figure 3). The line with the lowest minimum represents the best solution. This point can be more easily identified from the derivative of the TSI function. The point at which dTSI/dT = 0 defines the minimum point in the TSI plot. An example of this is shown in Figure 6.

The zero-point for this sequence of dTSI/dT plots is used to determine the amount of CO_2 needed to reach the minimum possible saturation index over a 2-D range of CO_2 and temperature. This is shown graphically in Figure 7, where the y-axis represents the set of points where a plot of TSI versus temperature is at a minimum.

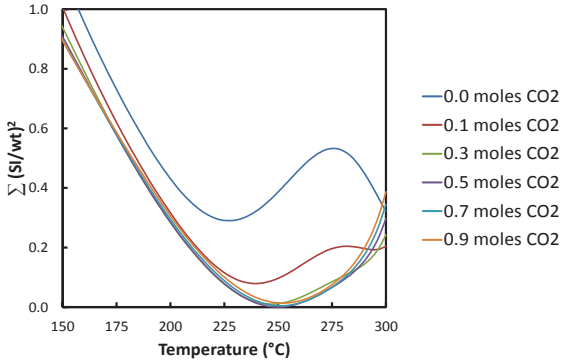

Figure 5: Plot of the total saturation index (TSI) as a function of temperature and added CO_2 for a shallow water sample derived from a deep geothermal reservoir that has lost volatiles as per Case 1 (e.g. Figures 3, 4).

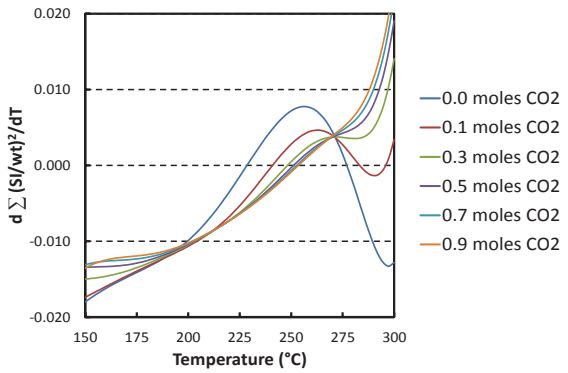

Figure 6: Plot of dTSI/dT as a function of temperature and added CO_2 for the same case as in Figure 5.

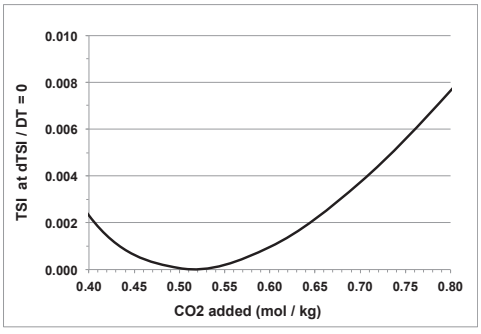

Figure 7: Plot of TSI at the point where dTSI/dT = 0 for all amounts of CO_2 added for the same case as in Figures 5 – 6.

The minimum of this value, when plotted against CO_2 added, yields a minimum point for CO_2 added, over the entire set. This minimum point for CO_2 added is then used to calculate the corresponding temperature value, as shown in Figure 8.

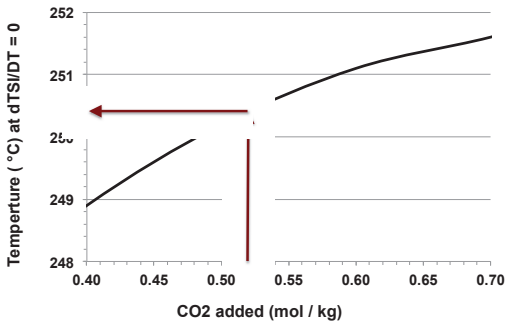

Figure 8: Plot of temperature at the point where dTSI/dT = 0 for all amounts of CO_2 added for Case 1 (e.g. Figures 3 – 7).

For Case 2, which incorporated the impact of typical analytic error, application of this inverse optimization method for geochemical modeling independently predicted reservoir temperature to within ± 3 °C. This result suggests that typical analytical errors can be tolerated in geothermometry.

The results for Test Case 3 (deep boiling) and Test Case 4 (flashing) are also encouraging for cases where there was water loss due to boiling. When the optimum value of TSI was at an approximate minimum with respect to mass of water loss, as estimated by selecting the temperature prediction for the water loss case with the lowest TSI at the optimum point, the method predicted the correct result to within ± 1 °C. Interestingly, the method selected an optimum point at no water loss for the deep boiling case (Case 3), and at 20% water loss for the steam flashing case (Case 4). In both instances, the actual amount of water loss was 15%. In Case 3, there is mass transfer due to the mineral equilibria, but no mass transfer in Case 4. This suggests that, if the extent of water partitioning can be independently measured (e.g., via isotopic techniques), then comparison of predicted and actual mass loss may provide a way to estimate the extent to which mineralization occurs within the geothermal system.

A comparison of results of the multicomponent geothermometry approach with some traditional geothermometers is provided in Table 4. The quartz geothermometer underestimates the reservoir temperature by as much as 80°C, while the Na-K geothermometers overestimate the reservoir temperature by 13 to 22 °C. In contrast, the multicomponent geothermometry method consistently estimates reservoir temperature to within ± 1 – 3 °C when water loss is taken into account.

Table 4: Comparison with temperature estimates using traditional geothermometers. Same cases as for Table 3.

Method	Case 1 T (°C)	Case 2 T (°C)	Case 3 T (°C)	Case 4 T (°C)
Inverse Modeling	251	253	250	249
[1] Fournier Quartz (no steam)	183	184	182	194
[1] Fournier Quartz (max steam)	170	172	170	180
[1] Fournier Chalcedony	156	157	156	168
[1] Fournier Am-SiO_2	59	60	59	70
[2] Fournier Na-K	271	263	270	271
[3] Giggenbach Na-K	272	265	272	272

[1] Truesdell and Fournier (1977)
[2] Fournier et. al. (1979)
[3] Giggenbach (1988)

SUMMARY AND CONCLUSIONS

The basic concepts of geothermometry have been available for about five decades and many of the early geothermometers are still being applied today. The application of these techniques can result in a wide range of estimated reservoir temperatures and limited ability to judge the uncertainty of the calculations. In this paper, we have proposed a multicomponent geothermometry technique that is an extension of the concepts provided by Reed and Spycher (1984). We take advantage of the advances that have been made in geochemical modeling, thermodynamic databases, and optimization tools to improve the estimates of reservoir temperatures.

To test these concepts, we have used The Geochemist's Workbench® to simulate the chemical composition of geothermal waters following cooling, loss of water vapor, loss of volatile constituents and mineral reactions. These simulations were then used to demonstrate our ability to replicate the initial reservoir temperatures. The results indicate that the

multicomponent geothermometry presented here has excellent potential for improving the practice of geothermometry for geothermal exploration and resource characterization. These preliminary results indicate that most geothermometry problems can be usefully resolved if the following factors are properly accounted for:

- Selection of the appropriate number of mineral phases to control solution equilibrium.
- Accurately selecting which minerals to use for geochemical calculations, on the basis of regional geology.
- Properly accounting for the impact of steam-water partitioning on solution chemistry.
- Properly accounting for the impact of the loss of volatile components on solution chemistry.

Typical analytical errors have only minimal effect on estimates of reservoir temperature. Overall, the results suggest that the multicomponent geothermometry method is relatively robust and could greatly improve the industry's ability to estimate deep reservoir temperatures. Additional improvements to the multicomponent geothermometry approach that are being explored include the use of other objective functions and alternative weighting functions, improved techniques for tracking gas phase partitioning, inclusion of additional volatile components (e.g., H_2S, H_2, CH_4), assessment of mineral reactions along the path from the deep reservoir and the sampling point, and methods for determining mineral assemblages. Extending this method beyond the relatively simple system explored via these simulations would require optimization of additional parameters and use of automated numerical optimization software that can conduct multi-component optimizations. This work is currently underway.

ACKNOWLEDGMENTS

Funding for this research was provided by the U.S. Department of Energy, Office of Energy Efficiency & Renewable Energy, Geothermal Technologies Program. We are also grateful to the Center for Advanced Energy Studies for providing additional support.

REFERENCES

Ármannsson, H. and Fridriksson, T. (2009), "Application of Geochemical Methods in Geothermal Exploration", *Short Course on Surface Exploration for Geothermal Resources*, organized by United Nations University Geothermal Training Programme, Ahuachapan and Santa Tecla, El Salvador, October 2009.

Bethke, C.M. and Yeakel, S. (2011), "The Geochemist's Workbench User's Guides, *Aqueous Solutions LLC,* Champaign IL.

Bethke, C.M. (2008), "Geochemical and Biogeochemical Reaction Modeling", Cambridge University Press, 2nd Ed., New York, New York, USA, 543 pp.

Doherty J. (2005), "PEST, Model-Independent Parameter Estimation User Manual, 5th Edition", Watermark Numerical Computing, www.pesthompage.org

Fournier, R.O., Sorey, M.L., Mariner, R.H., and Truesdell, A.H. (1979), "Chemical and Isotopic Prediction of Aquifer Temperatures in the Geothermal System at Long valley, California", *Journal of Volcanology and Geothermal Research*, **5**, 17-34.

Giggenbach, W.F. (1988), "Geothermal Solute Equilibria – Derivation of Na-K-Mg-Ca Geoindicators", *Geochimica et Cosmochimica Acta*, **52**, 2479-2765

Karingithi C.W. (2012), "Chemical Geothermometers for Geothermal Exploration", *Short Course V on Exploration for Geothermal Resources,* organized by United Nations University Geothermal Training Programme, Lake Bogoria and Lake Naivasha, Kenya, October 2010.

Reed, M.H. and Spycher, N.F. (1984), "Calculation of pH and mineral equilibria in hydrothermal waters with application to geothermometry and studies of boiling and dilution", *Geochimica et Cosmochimica Acta*, **48**, 1479-1492.

Schwartz, G.M. (1959), "Hydrothermal Alteration", *Economic Geology*, **54**, 161-183

Spycher, N.F., Sonnenthal, E. and Kennedy, B.M. (2011), "Integrating Multicomponent Chemical Geothermometry with Parameter Estimation Computations for Geothermal Exploration", *GRC Transactions*, **35**, 663-666.

Truesdell, A.H. and Fournier, R.O. (1977), "Procedure for Estimating Temperature of a Hot-Water Component in a Mixed Water by Using a Plot of Dissolved Silica versus Enthalpy", *Journal of Research of the U.S. geological Survey*, **5**, 49-52.

U.S. Department of Energy (2011), "Exploration Technologies, Technology Needs Assessment," *Energy Efficiency and Renewable Energy, Geothermal Technologies Program*, DOE/EE-0663.

Young, K., Reber, T., and Witherbee, K. (2012), "Hydrothermal exploration Best Practices and Geothermal Knowledge Exchange on OPENEI", *Proc. 37th Workshop on Geothermal Reservoir Engineering,* Stanford University, Stanford, CA, SGP-TR-194